DESIGN CONSIDERATIONS FOR THE APPLICATION OF ULTRA-HIGH-SLIP MOTORS TO BEAM PUMPING SYSTEMS

DONALD J. SIMON
Sargent Industries, Inc., Oil Well Equipment Division

Ultra-high-slip motors with speed variation capabilities in the range of 45% have been used on beam pumping installations for more than six years. As various producing companies started trying these motors, many improvements in system operation were noted, including:

1. Reduction in peak polished rod load
2. Increase in minimum polished rod load
3. Improved rod life
4. Reduction in peak torque by the API Torque Factor Method
5. A greatly altered dynamometer card shape which showed a tendency to approach the rectangular or parallelogram configuration
6. More production at the same strokes per minute
7. Greatly reduced current (ampere) peaks
8. Greatly reduced RMS (thermal) ampere requirement with a resulting improvement in power factor
9. A much steadier energy (kilowatt) requirement with frequent reductions in total kwh required.
10. Reduced distribution system voltage drop
11. Slower and smoother start-up of the pumping system with a visual recognition that its start-up was less strain on all components of the system
12. A greatly reduced start-up current demand which reduced the possibility of voltage collapse from heavy system loading.

These dramatic results created much enthusiasm among those who were involved with the operation and use of the motor. It was assumed by some that all these dramatic results would be obtained on every well in every condition, but that was not the case. On some wells no improvement in dynamometer card shape or rod loading was noted with no apparent improvement in torque loading on the gear box. These tests, which were seemingly failures, caused many interested industry people to doubt the value of an ultra-high-slip motor. Some even stated that it had no value or was detrimental to the system. Many heated and enlightening discussions ensued which contributed greatly to the present understanding of the total system operation.

An ultra-high-slip motor always improves the following factors on all pumping systems when operating at a significant (20% or more) speed variation:

1. All electrical characteristics are improved. Capacitors are normally disconnected when measuring power factor and ampere loading of a motor.
2. A significant reduction in peak torque and torque range, when the unit is properly counterbalanced, is always realized—with one minor exception. An air-balanced unit operating at very slow speed with no significant dynamic rod load will not realize a torque reduction.
3. The ultra-high-slip motor is effective in achieving these improvements on all crank counterbalanced units of both API and special design, and on all air-balanced units. It has no special value on an hydraulically actuated unit.

Studying the API RP11L series of bulletins has contributed greatly to an understanding of the operating conditions that will achieve major improvements in the mechanical load conditions of dynamometer card shape, peak and minimum polished rod load, torque reductions by the API torque factor method, increased pump plunger travel, and improved rod life.

To properly understand why load conditions change so dramatically with an ultra-high-slip motor, we must first see how the rotational speed of the pumping unit is altered by high speed variation. Figure 1(a) represents a typical crank arm speed curve for one cycle when driven by a typical Nema D motor. The speed variation is approximately 10%. The unit is balanced causing the slowest speed to be equal in the up and down strokes. Figure 1(b) represents a similar crank arm speed curve with the same average speed or strokes per minute, but with approximately 30% speed variation from an ultra-high-slip motor. This is also a balanced condition. Speed variation is defined as:

$$\frac{(\text{Maximum Speed - Minimum Speed})\ (100)}{\text{Maximum Speed}} = \text{Percent Speed Variation}$$

Where: Maximum Speed = Highest rpm or SPM
Minimum Speed = Lowest rpm or SPM

With high speed variation, pumping speed is increased considerably at each end of the stroke and is reduced considerably during the middle portions of the upstroke and downstroke.

Figure 2(a) represents the polished rod velocity curve resulting from the rotational speed curve of Fig. 1(a) on an API pumping unit. This curve is a direct function of the geometry of the pumping unit with minor variations due to the slight speed change. Figure 2(b) represents the polished rod velocity curve on the same unit resulting from the rotational speed variation of Figure 1(b). The polished rod velocity curve is radically altered from that of the geometry induced curve. It should be noted that the abscissa of these curves is time. Therefore, the slope of the curves is acceleration. Since force equals mass times acceleration, it follows that increased acceleration would tend to increase force, and decreased acceleration would tend to decrease force. Force is the polished rod load as measured by the dynamometer. The mass involved in the above equation is the *EFFECTIVE instantaneous* mass which is a result of the spring action of the rod string and other factors such as fluid load or buoyancy, damping, natural frequency, friction, and harmonic effects of previous forces applied throughout the rod string. By comparing Fig. 2(b) to Fig. 2(a) we can readily see that the acceleration of the ultra-high-slip motor operation is increased at the beginning of the upstroke which causes an increase in polished rod load early in the upstroke.

Figure 3(a) is a dynamometer card resulting from the velocity curve of Fig. 2(a). Figure 3(b) is the dynamometer card resulting from the velocity curve of Fig. 2(b) on the same well, operating, as nearly as possible, at the same conditions. The polished rod load is heavier at the beginning of the upstroke. The rod load during the middle portion of the upstroke is flatter with a reduced peak load because the velocity curve is relatively constant with minimal acceleration. In this particular case the peak load was reduced by 2369 lb. This represents a 36.6% reduction in the Peak Polished Rod Load Factor (F_1 of API RP-11L). Continuing with the study of Figs. 2 and 3, note that the deceleration at the end of the upstroke is greater for the ultra-high-slip operation which would tend to cause a lighter load. In this case the load is heavier because of greater effective mass, which will be explained a little later. With the faster downward acceleration at the beginning of the downstroke one would expect a lighter load. This is the case. With the flat velocity curve during the middle portion of the downstroke and its minimal acceleration, an increased load would be expected, which is the case. In this example, the minimum polished rod load was increased by 1105 lb, which results in a 24.1% reduction in the Minimum Polished Rod Load Factor (F_2 of API RP-11L). Near the end of the downstroke, the increased deceleration of the ultra-high-slip operation would tend to cause an increased rod load; but, again, this was not the case because of a changed effective mass.

Both dynamometer cards of Fig. 3 are good visual examples of the effect caused by the natural frequency of the rod string and the non-dimensional pumping speed of the API RP-11L calculations. The second half of the upstroke and downstroke tend to be mirror reflections of the first half of the up and down strokes. This frequency condition is what made the effective mass dominate as factor of load at each end of the stroke instead of acceleration.

When a pumping system is operating at

relatively slow nondimensional pumping speed there is little an ultra-high-slip motor can accomplish at the dynamometer. Figures 4(a) and 4(b) represent this type of operational comparison. The ultra-high-slip motor might increase the load range slightly. However, there can still be a large actual reduction in peak torque at the gear box due to the inertial help of the counterweights in a 35-45% slow-down. The API RP-11L method ignores surface equipment inertia entirely.

The area of a dynamometer card's trace represents work. The ultra-high-slip motor operation has increased work accomplished at each end of the stroke and decreased work during the middle of the stroke. Increased work at the ends of the stroke is accomplished by increased pump plunger travel due to overtravel effect. Generally, increased nondimensional pumping speed results in increased pump plunger travel due to the overtravel effect. An ultra-high-slip motor is operating at faster than the average speed at the ends of the stroke with an increased nondimensional pumping speed. In the two comparisons of Fig. 3, the gross plunger travel was increased by at least 10%. Rod load range was reduced by 31.4%.

Figures 5(a) and 5(b) are reproductions from page 27 of API Bulletin 11L2, First Edition. They represent identical pumping conditions with the exception that Fig. 5(a) represents 0% slip drive while Fig. 5(b) represents 10% slip drive. By carefully scaling these cards, we find that the 10% slip card indicates a reduction of 8.1% for the Peak Polished Rod Load Factor (F_1), a reduction of 22.2% for the Minimum Polished Rod Load Factor (F_2), and a reduction in range of load of 12.7%, when compared to the 0% slip card.

It should also be noted that in Fig. 5(a), negative work (reduced plunger travel) is indicated at the bottom of the stroke while essentially no work is indicated at the bottom of the stroke in Fig. 5(b). At the top of the stroke of Fig. 5(a) no work is being accomplished while positive work is being accomplished at the top of the stroke of Fig. 5(b). The 10% slip drive accomplished more work at the ends of the stroke similar to the examples of Fig. 3. Similar variations due to slip are evident throughout Bulletin 11L2.

During the late 1950's and early 1960's it was the general consensus of opinion that prime mover slips in excess of 5-8% would not be of any benefit to a pumping unit system. Those who held this opinion had neither ultra-high-slip prime movers nor instrumentation for proper evaluation. Since force equals mass times acceleration, it is theoretically possible to maintain constant upstroke and downstroke forces by maintaining a proper combination of effective mass and acceleration. This is almost achieved when nondimensional rod stretch and nondimensional pumping speed are very low. The high speed variation capability of an ultra-high-slip motor tends to approach this theoretical ideal.

By mathematical extrapolation and field test verification, we have been able to develop sets of curves as an addendum to the API RP-11L curves for all ranges of expected speed variations up to 45%. The present API curves are good for speed variations of from 0-10%. The three new sets of curves are for speed variations of 15-25%, 25-35%, and 35-45%. These new sets of curves reflect the expected changes for pump plunger travel, peak polished rod load, minimum polished rod load, peak torque, and polished rod horsepower. We do not consider a revision of the Torque Adjustment curve necessary. It should also be noted that the new Peak Torque curves reflect only the torque reduction caused by load range reduction; they do not reflect the very significant reduction in torque at the gear box due to the energy furnished by the inertia of all masses between the polished rod and the gear box. These new sets of curves have the same limitations of variance from subsurface friction, API pumping unit geometry, and other abnormal conditions as the standard API RP-11L design curves.

For purposes of brevity, we will compare the 0-10% speed variation curves of the conventional motor operation to the 35-45% curves of ultra-high-slip operation. These comparisons will be for 0.3 as the nondimensional rod stretch and 0.3 as the nondimensional pumping speed. Complete sets of curves for all ranges of speed variation of convenient size and form are available from the author in reasonable quantities at no charge.

Figures 6(a) and 6(b) compare the Plunger Stroke Factors. At the nondimensional conditions mentioned previously, the plunger stroke has been increased by 18.5%. The Peak Polished Rod Load Factors of Figs. 7(a) and 7(b) indicate a reduction of 12.6%. The Minimum Polished Rod Load Factors of Figs. 8(a) and 8(b) indicate a reduction of 20.1%. This results in an increased minimum load. The Peak Torque Factors of Figs. 9(a) and 9(b) indicate a peak torque reduction of 14.7%. The Polished Rod Horsepower Factors of Figs. 10(a) and 10(b) indicate an increase of 9.2%. Table 1 is a tabulation of percent change of all these factors at various combinations of nondimensional pumping speed and rod stretch. It includes a percent load range change at the bottom of the table. A percentage change by use of an ultra-high-slip may be predicted for any of the combinations of speed variation and for all of the factors by use of the following formula:

$$\frac{(\text{UHS Factor - Conv. Factor})\ (100)}{\text{Conv. Factor}} = \%\ \text{change}$$

It should be noted that a positive (+) change for the Plunger Stroke Factor is an improvement, while all the other factors should be negative (-) for an improvement. The increase in plunger travel should be considered with an increase in Polished Rod Horsepower.

Tests have indicated these curves are on the conservative or safe side for design purposes. In actual operation far better results than these curves predict are usually achieved.

The author believes that an industry-wide investment in reactivating the studies performed by the Midwest Research Institute would bring profitable returns with improved producing capability and efficiency at higher volumes from deeper wells. These new studies should include speed variations up to 45% with counterbalance variations of 30% from the balanced condition. It should also include a thorough study of the inertial effects of the moving parts of a pumping unit and prime mover.

Ultra-high-slip motors with their very soft torque output and wide speed variation capability must *always* tend to reduce mechanical, electrical, and hydraulic peaks within the system.

BIBLIOGRAPHY

1. API RP-11L, Second Edition, March 1972, "Recommended Practice For Design Calculations For Sucker Rod Pumping Systems (Conventional Units)."
2. API BUL 11L2, First Edition, December 1969, "Catalog of Analog Computer Dynamometer Cards."

ACKNOWLEDGMENTS

The author wishes to thank the following for their interest and assistance in helping develop the understanding of ultra-high-slip motor operation to its current level.

Mr. Ed Aldridge—Amoco Petr. Co.—Odessa, Texas

Mr. Joe Chastain—A.L.E.S.—Midland, Texas

Mr. Bob Gault—Bethlehem—Midland, Texas

Mr. Sam Gibbs—Nabla Corp.—Midland, Texas

Mr. Fred Gipson—Conoco—Houston, Texas

Mr. John Hughes—Shell Oil Co.—Midland, Texas

Mr. I.W. Hynd—Retired—Midland, Texas (He started it all)

Mr. Doug Patton—Corod—Denver, Colorado

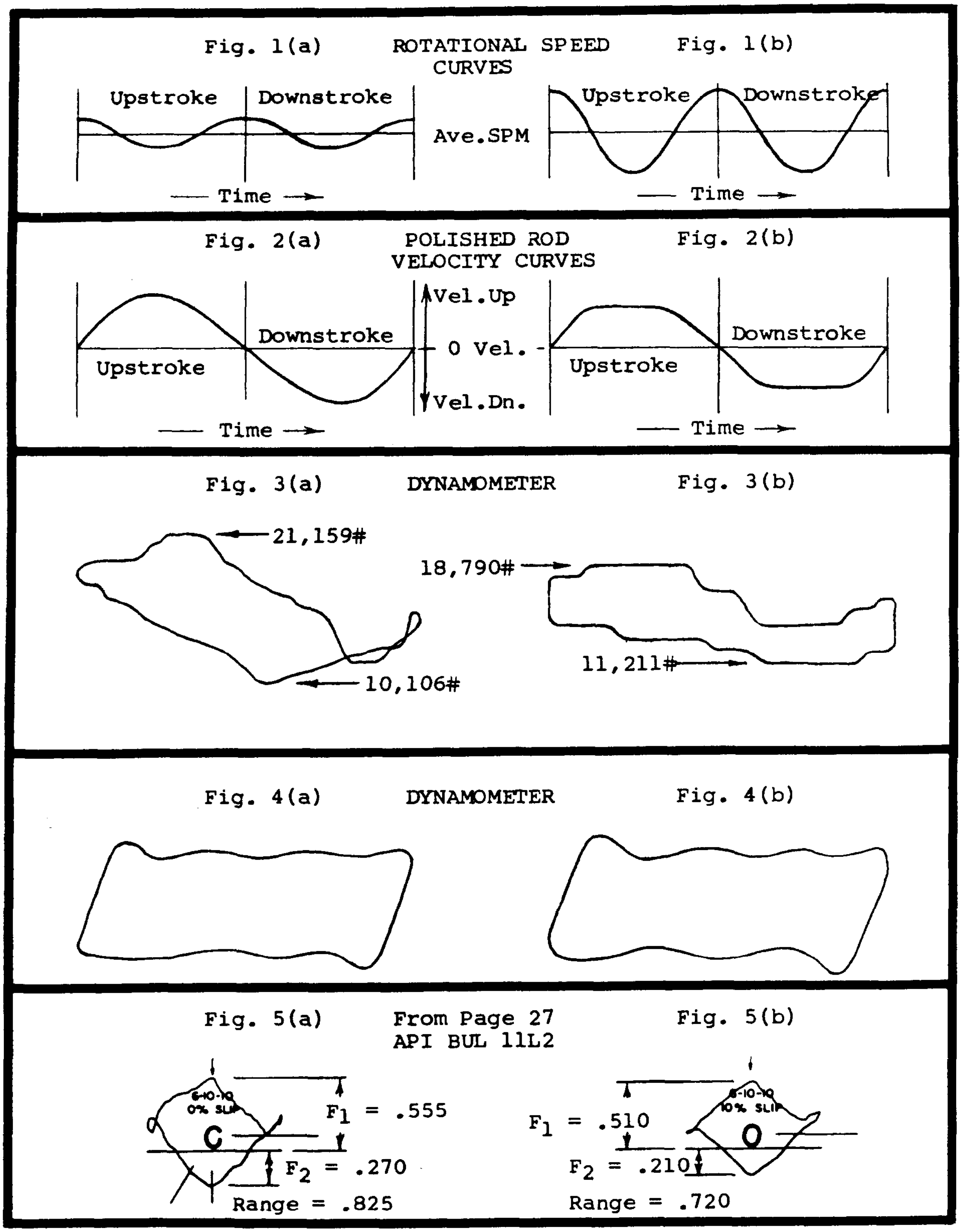
Fig. 1(a)
ROTATIONAL SPEED CURVES
Fig. 1(b)
Upstroke
Downstroke
Ave.SPM
Time
Upstroke
Downstroke
Time
Fig. 2(a)
POLISHED ROD VELOCITY CURVES
Fig. 2(b)
Upstroke
Downstroke
Vel.Up
0 Vel.
Vel.Dn.
Time
Upstroke
Downstroke
Time
Fig. 3(a)
DYNAMOMETER
Fig. 3(b)
21,159#
10,106#
18,790#
11,211#
Fig. 4(a)
DYNAMOMETER
Fig. 4(b)
Fig. 5(a)
From Page 27
API BUL 11L2
Fig. 5(b)
F1 = .555
F2 = .270
Range = .825
F1 = .510
F2 = .210
Range = .720

FIGS. 1(A)-5(B)

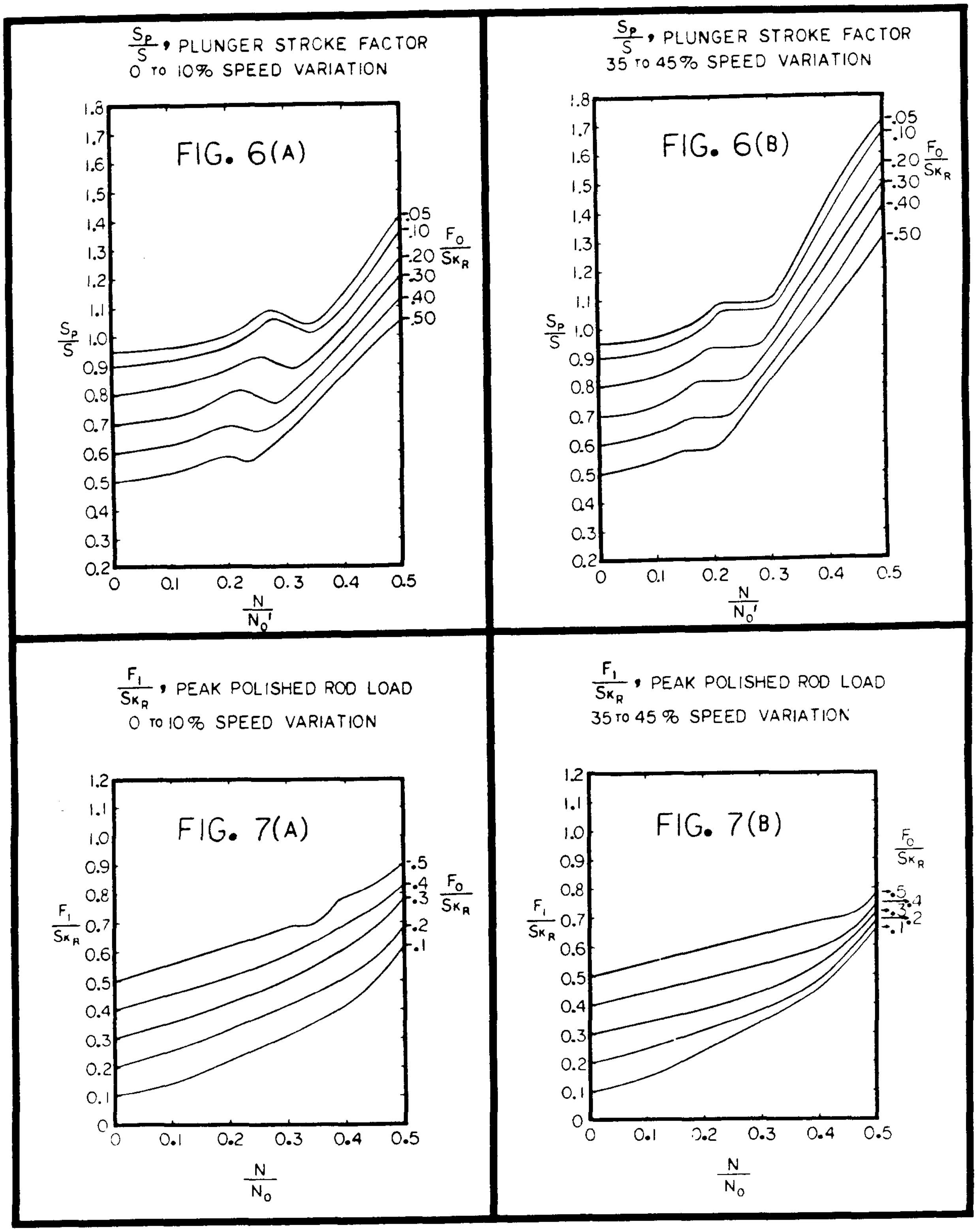
Sp/S, PLUNGER STROKE FACTOR
0 TO 10% SPEED VARIATION
FIG. 6(A)
Sp/S
N/No'
Fo/SKR
.05
.10
.20
.30
.40
.50
Sp/S, PLUNGER STROKE FACTOR
35 TO 45% SPEED VARIATION
FIG. 6(B)
F1/SKR, PEAK POLISHED ROD LOAD
0 TO 10% SPEED VARIATION
FIG. 7(A)
F1/SKR
N/No
F1/SKR, PEAK POLISHED ROD LOAD
35 TO 45% SPEED VARIATION
FIG. 7(B)

FIGS. 6(A)-7(B)

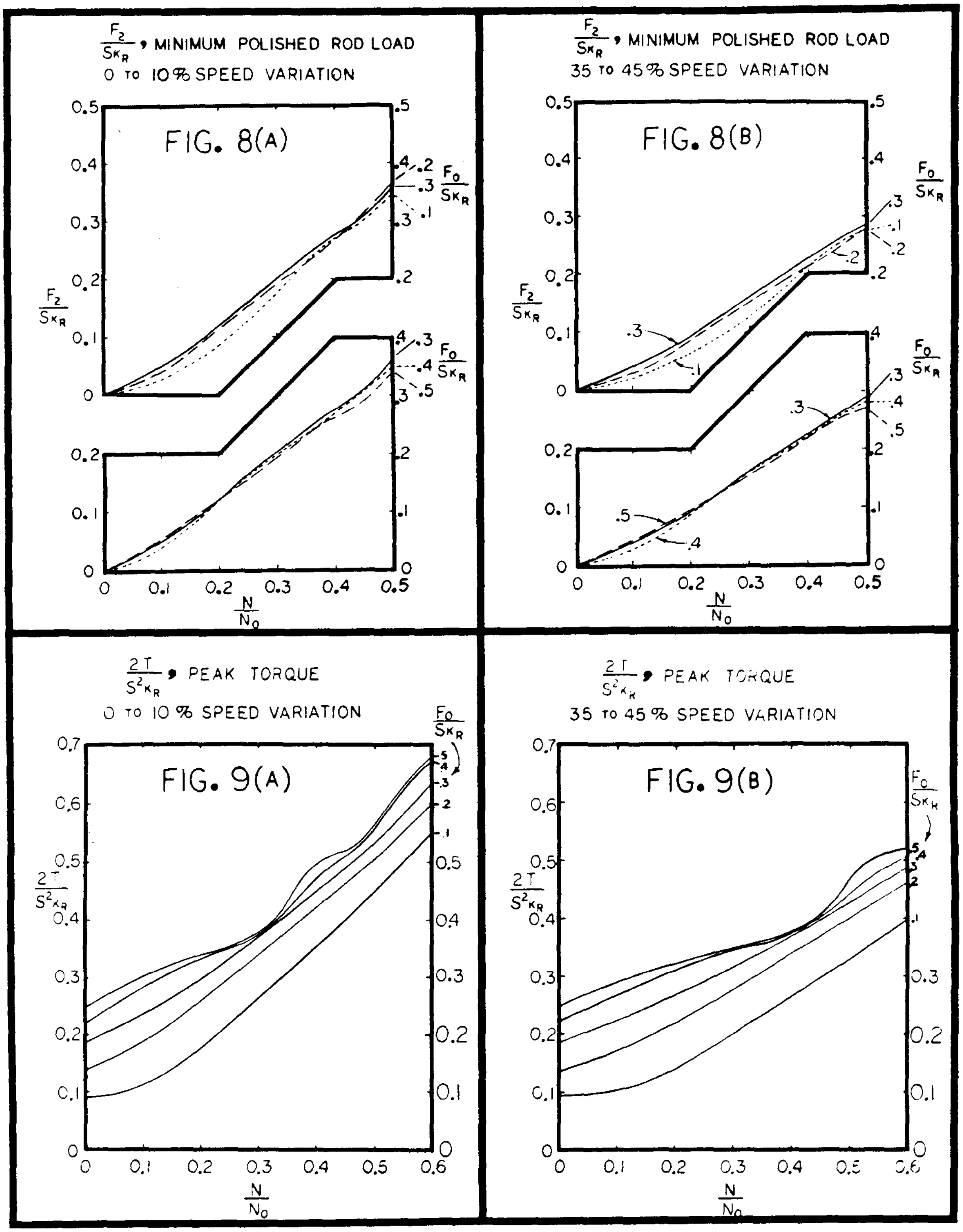

F2/SKR, MINIMUM POLISHED ROD LOAD
0 TO 10% SPEED VARIATION
FIG. 8(A)
F2/SKR, MINIMUM POLISHED ROD LOAD
35 TO 45% SPEED VARIATION
FIG. 8(B)
F0/SKR
N/N0
2T/S²KR, PEAK TORQUE
0 TO 10% SPEED VARIATION
FIG. 9(A)
2T/S²KR, PEAK TORQUE
35 TO 45% SPEED VARIATION
FIG. 9(B)

FIGS. 8(A)-9(B)

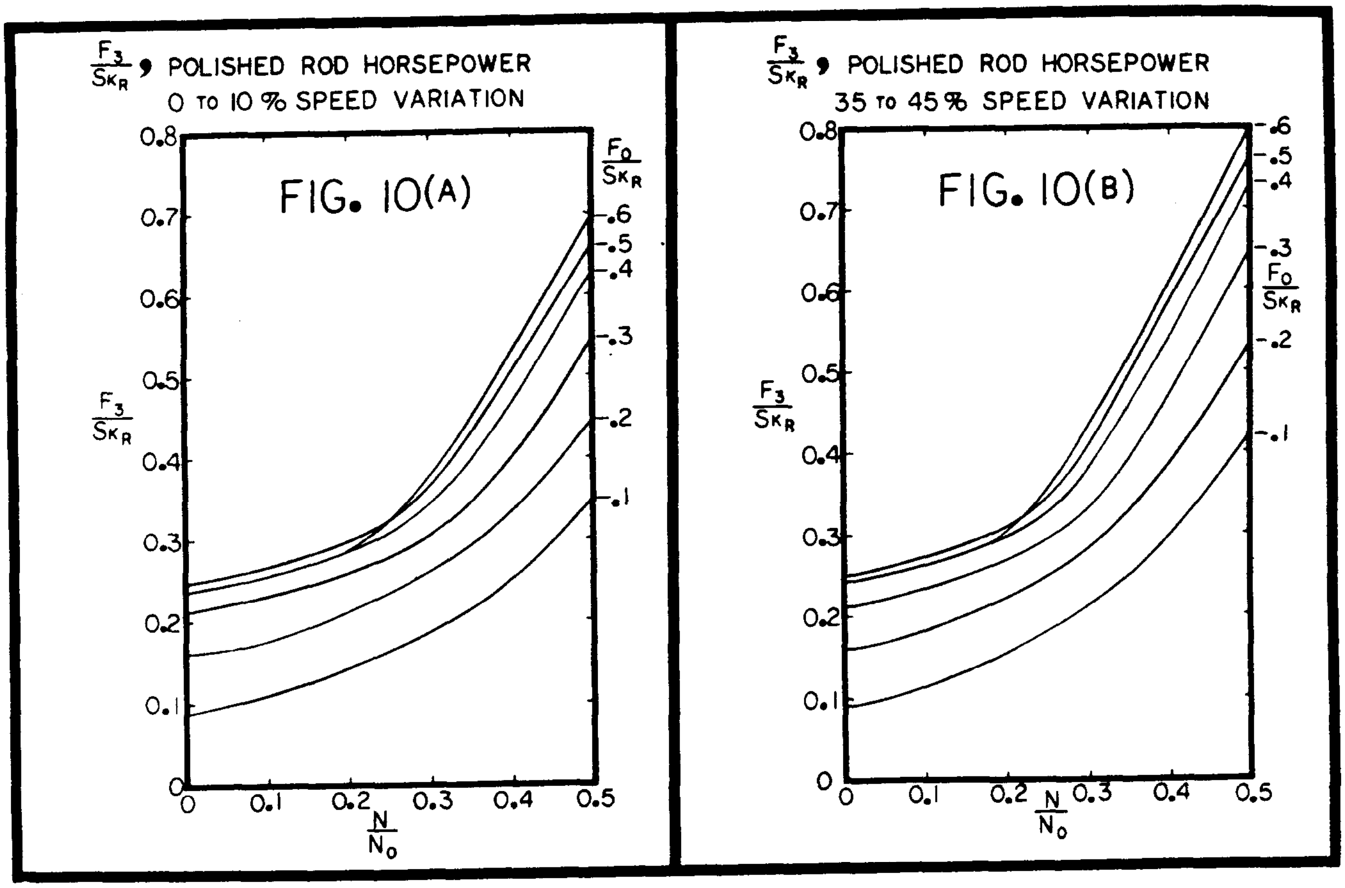

FIG. 10

TABLE 1—PERCENT CHANGE OF FACTORS BETWEEN 35-45% CURVES AND 0-10% CURVES

N/No or N/No	.1	.1	.2	.2	.2	.3	.3	.3
Fo/Sk$_r$	.1	.3	.2	.3	.4	.2	.3	.4
Plunger Stroke Factor	+.8%	+1.4%	+5.2%	+1.9%	0%	+9.7%	+18.9%	+20.8%
PPRL Factor	+4.2%	-4.8%	-5.8%	-9.4%	-6.5%	-8.4%	-12.5%	-8.8%
MPRL Factor	-25.9%	-18.0%	-25.4%	-23.8%	-29.5%	-20.9%	-20.5%	-20.0%
Peak Torque Factor	-6.3%	-6.7%	-15.5%	-11.0%	-6.9%	-18.3%	-10.3%	-8.3%
PRHP Factor	+2.7%	+1.7%	+4.5%	+3.1%	+3.1%	+9.6%	+7.7%	+12.4%
Load Range Change (Not API Calc.)	- .6%	-6.4%	-10.8%	-12.6%	-10.9%	-12.4%	-14.8%	-11.7%